that GAK acts not only in the cytoplasm but also in the nucleus.

Another putative novel role of GAK appears to be played by its association partners, cyclin G and protein phosphatase 2A (PP2A) B'α subunit that are partially localized in the nucleus. It has been shown that PP2A is recruited to its target proteins by cyclin G1 (Okamoto *et al.* 1996), a member of the cyclin family (Tamura *et al.* 1993). The cyclin G1 gene is a target of the p53 tumor suppressor protein (Okamoto & Beach 1994) and is induced in a p53-dependent manner in response to DNA damage (Kimura & Nojima 2002). Cyclin G1 was found to complex with and regulate the active PP2A holoenzymes and control MDM2 by dephosphorylating its T216 and S166 residues; this leads to the destabilization of p53 (Okamoto *et al.* 2002). Moreover, cyclin G1 interacts directly with MDM2 after DNA damage and promotes ARF/MDM2 complex formation, thereby downregulating p53 levels; indeed, the accumulation of p53 that is observed after DNA damage was enhanced in cyclin G1−/− cells (Kimura & Nojima 2002), even though the cyclin G1 null mouse is normal at birth and remains healthy in adulthood (Kimura *et al.* 2001). These findings suggest that cyclin G1 is a key regulator of the p53-MDM2 network that acts in part in the nucleus by regulating PP2A (Chen 2002).

PP2A is one of the highly abundant and ubiquitously expressed Ser/Thr phosphatases that regulate multiple signaling pathways in eukaryotic cells (Janssens *et al.* 2005; Westermarck & Hahn 2008). PP2A consists of three subunits, namely, invariable catalytic (C) and structural (A) subunits and a variable regulatory (B) subunit. Three unrelated PP2A regulatory subunit families denoted as B, B′ and B″ have been identified. With regard to the B′ family, these are encoded by five distinct mammalian genes. Moreover, many isoforms are generated from these genes. Of relevance to this paper is the B′α (alternatively called B56gamma) subunit subfamily, which includes three alternative splicing variants with differing subcellular localizations (Ito *et al.* 2000), namely, either in the nucleus (B′α1 and B′α2) or in the cytoplasm (B′α3). Hereafter, we will sometimes refer to PP2A B′α simply as B′α.

Thus, it is apparent that GAK, at least partly, plays a role in the nucleus. Nonetheless, no direct evidence for the nuclear activity of GAK has been reported to date. In the present study, we show that GAK localizes not only in the cytoplasm but also in the nucleus, where it complexes with nuclear proteins such as p53, clathrin heavy chain (CHC) and B′α1, a nuclear form of the B′α subunit. Moreover, we show here that association domains between GAK and CHC are distinct from cytoplasm and nucleus.

Results

GAK localizes in both the cytoplasm and nucleus

Reflecting its role as a regulator of clathrin-mediated membrane trafficking, GAK localizes in the cytoplasm (Greener *et al.* 2000), in particular at the *trans*-Golgi network (TGN; Kametaka *et al.* 2007). When we examined the localization of GAK by immunofluorescence with a polyclonal anti-GAK antibody (pGAK) or a monoclonal anti-GAK antibody (1E1) that we prepared previously (Kanaoka *et al.* 1997) using laser scanning microscope (Fig. 1A,B), we could show that at least some immunostained images are detected as the filamentous structure in human cells such as HEF (human embryonic fibroblasts), KD (a primary culture of human lip fibroblasts) and HeLa (cervical cancer). Moreover, we always observed not only the filamentous images in the cytoplasm, but also the dotted images in the nucleus (Fig. 1A,B); indeed, the nuclear signals detected here were stronger than the cytoplasmic signals when 1E1 monoclonal antibody was used (Fig. 1B).

Because the 1E1 monoclonal antibody is not useful for Western blot analysis due to its low sensitivity, we prepared new monoclonal antibodies against GAK and found that two of the clones denoted as 9–10 and 9–13 detected purified GAK specifically and with high sensitivity (Fig. 1C). They also both detected a doublet of bands in HeLA S3 cell extracts around 170 kDa (Fig. 1C). When we immunostained TIG-1 cells with these monoclonal antibodies, we found that clone 9–10 only detected nuclear GAK while clone 9–13 detected GAK in both the nucleus and cytoplasm (Fig. 1D). As expected, most of the dotted images in the nucleus and the filamentous images in the cytoplasm that were obtained by immunostaining with the polyclonal antibody pGAK and the 9–10 and 9–13 monoclonal antibodies overlapped almost completely (Fig. 1D). These results confirmed by one polyclonal antibody and three distinct monoclonal antibodies indicate that GAK also localizes in the nucleus, even though GAK does not appear to have a nuclear localization signal (NLS). When we performed siRNA-mediated knockdown experiment to examine if these nuclear signals were reduced by depletion of GAK mRNA, we found that the GAK-knockdown cells showed the cell cycle arrest at metaphase when nuclear membrane was lost (our unpublished result); thus, it was unable to analyze the status of nuclear localization of GAK under these conditions.

Because the filamentous images of GAK in the cytoplasm (Fig. 1A,B,D) resembles those of endoplasmic reticulum (ER) or mitochondria, we stained the human TIG-1 cells (human fetal lung fibroblasts) with the ER

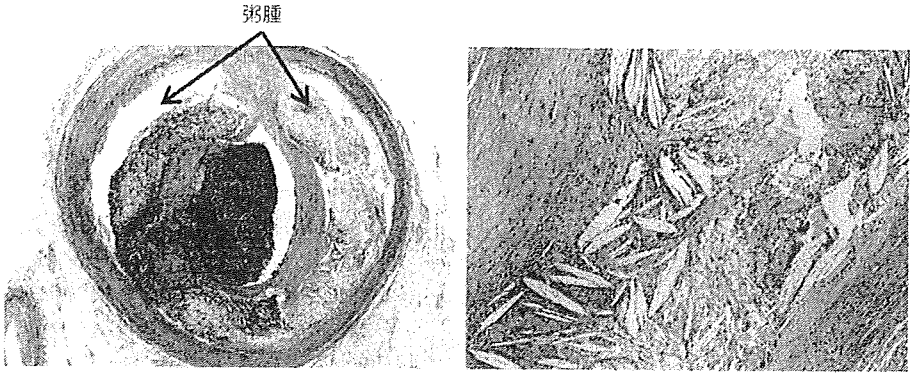

図❺ 不安定プラークの破綻により生じた血栓性内腔閉塞，77 歳男性，RCA

学的要因，内皮細胞機能異常などさまざまな因子が加って動脈の再構築が継続し，新たな閉塞性病変や再疎通，石灰化など，患者の予後を左右する二次的な変化がもたらされる．

一方，一般にいう動脈硬化症とはアテローム性動脈硬化症を意味する．本疾患は動脈壁の損傷により血管壁内へ脂質をはじめとする血漿成分が浸み込むことにより生じる病態である．病理組織学的にはその進行度により脂肪線条，線維性プラーク，複合病変に大別される．複合病変とはもっとも進行した病変であり，粥腫の破綻，それにもとづく出血や血栓形成，石灰化などを伴う．さらに，脂質に富むプラークとそれを覆う脆弱な線維組織とからなる不安定プラークの破綻が虚血性心疾患の発症に大きく関与することも指摘されている（図❺）．

このように後炎症性動脈硬化症である川崎病後遺症とアテローム性動脈硬化症とは発生機序の面からも病理組織像からも大きく異なるものであり，動脈壁障害や内皮細胞障害といった観点のみから動脈硬化症として同一に扱うことには慎重でなければならない．

○ 後炎症性動脈硬化症はアテローム性動脈硬化症の危険因子になりうるか

後炎症性動脈硬化症とアテローム性動脈硬化症とは本質的に異なることを述べてきたが，川崎病の報告から 40 年以上が経過した現在，初期に川崎病に罹患した患者はすでに中年期を迎えている．今後，川崎病の既往歴を有する中高年人口がますます増加することが見込まれる状況のなかで，血管炎後遺病変が脂質異常症や高血圧，糖尿病，喫煙などと同様にアテローム性動脈硬化症を加速する因子になり得るかどうか，明らかにされるべききわめて重要な課題である．

筆者らの施設に保存された遠隔期川崎病剖検症例の冠状動脈病変に対し，泡沫細胞などのアテローム性動脈硬化症で観察される所見について検索をおこない，これまでに報告されている日本人若年者のアテローム性動脈硬化症についての全国的な剖検調査成績[7]と比較した．この調査によると 40 歳未満の若年者で冠状動脈にアテローム性動脈硬化病変をみる頻度は低く，とくに複合病変については 10 代，20 代では出現せず，30 代でもその頻度は冠状動脈総面積の 1%に満たないという．比較検討の結果，瘤が残存した症例では年齢を合致させた非川崎病対照症例と比較して強いアテローム性動脈硬化症が観察されたが（図❻）[8]，他の再疎通血管や瘤非形成例の冠状動脈においてはこれまでのところ対照とのあいだに明確な差異を見出せていない[8]．

後炎症性動脈硬化症とアテローム性動脈硬化症との関連を明らかにすることはきわめて重要な課題ではあるが，いまだ一定の見解を得ていない．今後継続して慎重に議論されるべき問題点である．

○ おわりに

川崎病後遺症としての後炎症性動脈硬化症の病理形態像を中心に記載した．川崎病全国調査成績によれば 1970 年以前の川崎病登録患者の累計はおよそ 2,000 名である．

(or TGN) staining marker ER-Tracker™ Red and the mitochondrial staining marker MitoTracker™ Red to examine whether at least some of the cytoplasmic GAK colocalize with these cytoplasmic structures. We first confirmed that the cytoplasmic GAK partly localized at the TGN (Kametaka *et al.* 2007) or ER in TIG-1 cells (Fig. 1E, arrows). Moreover, we found that at least some of the immunostained images of GAK also coincided with those of mitochondria (Fig. 1F, arrowheads). Notably, no nuclear dot was observed when we skipped the permeabilization process with 0.1% Triton X-100 after the cell fixation (see Experimental procedures) to highlight the ER or TGN-staining with ER-Tracker™ Red (Fig. 1E); this is because the nuclear membrane remained intact to inhibit the entrance of anti-GAK antibody into the nucleus. Thus, Triton-treatment is essential to visualize the nuclear localization of GAK.

To examine whether these nuclear dots of GAK colocalize with nuclear bodies (NBs) that are recognized by antibodies against SF2 (nuclear stress bodies; Biamonti 2004; Chiodi *et al.* 2004), promyelocytic leukaemia (PML) protein (PML-NB; Bernardi & Pandolfi 2007), or coilin (Cajal body; Stanek & Neugebauer 2006), we immunostained TIG-1 cells using the relevant antibodies; however, we could detect no remarkable colocalization of GAK with these NBs (Supporting Fig. S1).

GAK is phosphorylated in the nucleus

To determine if GAK is modified by phosphorylation, we used human embryonic kidney 293T cells because they yield comparatively large amounts of cell extract per culture dish. Upon Western blot analysis of the 293T extract, the 9–10 and 9–13 antibodies revealed the same doublet of bands around 170 kDa (Fig. 2A) that were detected by these antibodies in HeLa S3 cell extracts (Fig. 1C). When we added λ-phosphatase to the 293T cell extract in the presence or absence of phosphatase inhibitors, the upper band that was detected by both the 9–10 and 9–13 antibodies migrated slightly faster; this effect was blocked when phosphatase inhibitors were also present (Fig. 2A). Ectopically expressed 6Myc-GAK showed similar band shifts, which indicates that exogenous GAK is also subjected to phosphorylation (Fig. 2B). Significantly, the kinase-dead form of GAK (M-GAK-KD) also showed similar band shifts (Fig. 2C). This indicates that GAK phosphorylation is not due to self-phosphorylation. Notably, the lower band of the doublets shown by asterisks in Fig. 2A disappeared when the insoluble materials were removed by centrifugation before the extract was dissolved in sample buffer for electrophoresis (Fig. 2B,C); this band may thus be a nonspecific background artifact or another modified form of GAK that is bound to the insoluble materials.

To confirm the nuclear localization of GAK biochemically, we isolated nuclear and cytoplasmic proteins from 293T cells and subjected them to Western blot analysis using 9–10, 9–13 and pGAK anti-GAK antibodies. The successful fractionation of the cell extract was confirmed by probing the Western blots with an antibody against the cytoplasmic protein α-tubulin or the nuclear protein origin recognition complex 2 (Orc2), although it should be noted there was slight contamination of the cytoplasmic fraction by nuclear proteins and *vice versa* (Fig. 2D-i). We also detected GAPDH as a loading control. Close examination of the area of the SDS-polyacrylamide gel around the molecular weight of 170 kDa revealed that all anti-GAK antibodies recognized multiple bands in both the cyoplasmic and nuclear fractions (Fig. 2D-ii, -iii and -iv). Because some of these multiple bands (denoted by arrows or arrowheads) were observed by using distinct antibodies, they probably showed the GAK bands but not the nonspecific background. For example, the lower band of the doublet bands (asterisk) was detected in the nuclear but not the cytoplasmic fraction, as were three

Figure 2 Western blot analysis of GAK and subcellular localization of GFP-GAK. (A–D) Western blot analysis of phosphorylation modifications of endogenous GAK (A) or ectopically expressed Myc-tagged wild-type GAK (M-GAK; B) or kinase-dead GAK (M-GAK-KD; C) in 293T cells by examining the effect of λ-phosphatase (PPase) and/or phosphatase inhibitors. GAK was detected by the 9–10 or 9–13 anti-GAK monoclonal antibodies (A) or the anti-Myc monoclonal antibody (B, C). The arrowsheads indicate the shifting of the band due to (de)phosphorylation. The asterisk in (A) denotes the lower band of the doublet bands (see Figs 1C and 2G). (D) Western blot analysis of cytoplasmic and nuclear fractions of 293T cell extracts using anti-Orc2 (nuclear control), anti-α tubulin (cytoplasmic control), or anti-GAPDH (loading control) antibodies (i) or 9–10 (ii), 9–13 (iii), or pGAK (iv) anti-GAK antibodies. Cyto, cytoplasmic fraction; Nuc, nuclear fraction. The arrows and small arrowheads indicate the bands detected specifically in the nuclear fraction alone and primarily in the cytoplasmic fraction, respectively. The large arrowhead and the asterisk denote the upper and lower bands of the doublet bands, respectively (see Figs 1C and 2A). The position of the 170 kDa sizemarker is shown by the horizontal bars. (E–G) Subcellular localization of GFP-GAK after its ectopic expression in HeLa cells. (E) Schematic depiction of plasmid constructs expressing intact GAK (GAK full), GAK-N (which contains the kinase domain), and GAK-C (which lacks the kinase domain). (F) Fluorescent images of GAK full, GAK-N, GAK-C or vector alone, as observed under a fluorescence microscope. Bar = 10 μm. (G) Western blot analysis of HeLa cell extracts expressing GAK full, GAK-N, GAK-C or vector alone by using anti-GFP antibody. Arrows indicate the intact, appropriately sized, GFP-fusion proteins.

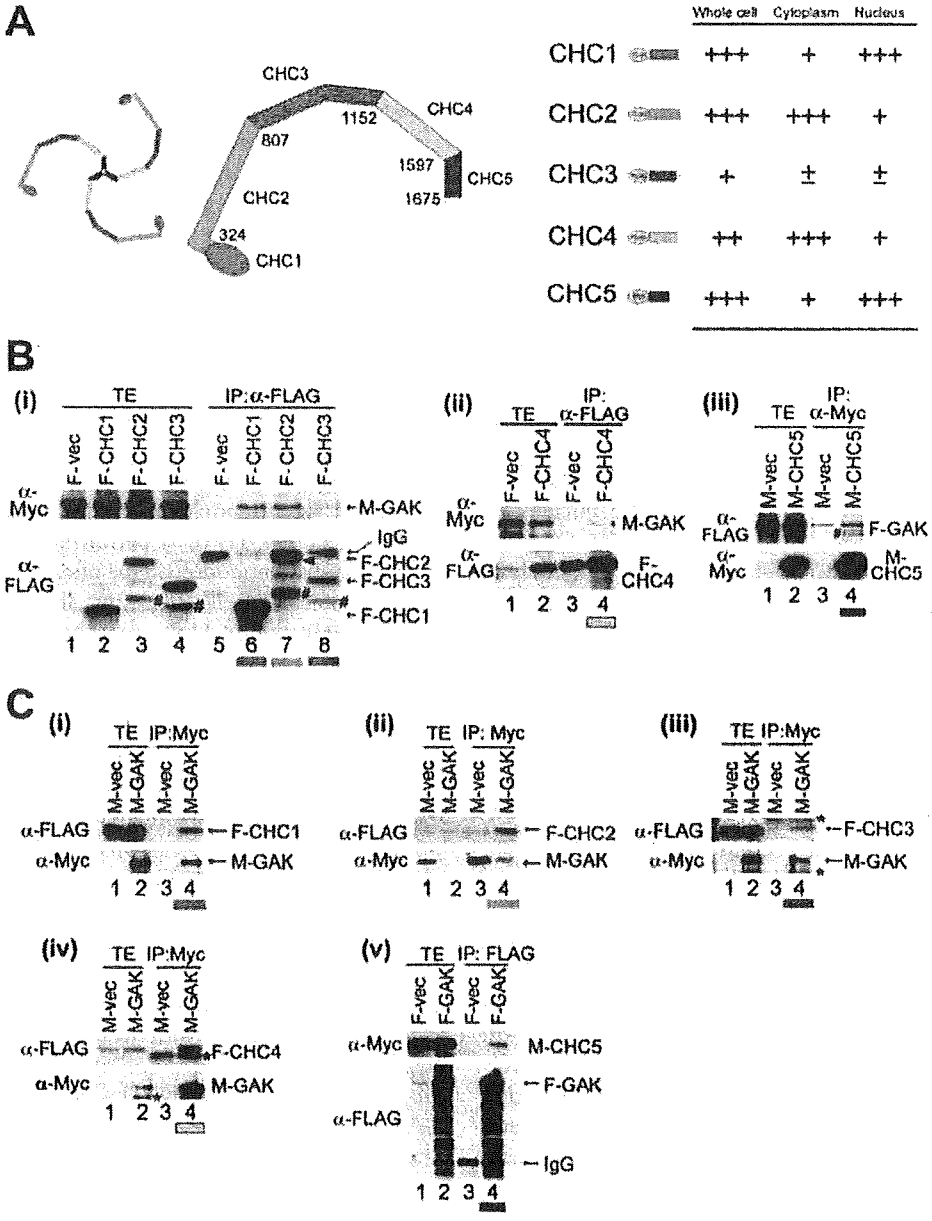

Figure 5 GAK associates with CHC through distinct domains in cytoplasm and nucleus. (A) Schematic depiction of the CHC fragments used in this study (left panels) and a summary of their ability to associate with GAK (right panel). CHC was dissected into five parts according to Edeling *et al.* (2006). GAK strongly associates with CHC2 (green) and CHC4 (yellow) in cytoplasm, while it associates with CHC1 (red) and CHC5 (blue) in nucleus. GAK associates only weakly with CHC3 (purple) in both cytoplasm and nucleus. Two or three pluses signify a stronger association. CHC1~4 were tagged (light blue ovals) with 3FLAG (F-CHC1~4) while CHC5 was tagged with 6Myc (M-CHC5). (B, C) GAK coimmunoprecipitates with CHC1, 2, 4 and 5. 293T cells were cotransfected with Myc- or FLAG-tagged GAK along with FLAG-CHC1~4 or Myc-CHC5. The total cell extract (TE) was directly subjected to Western blot analysis with anti-Myc and anti-FLAG antibodies (left panels). Alternatively, the extracts were immunoprecipitated (IP) with anti-FLAG or anti-Myc antibody and the immunoprecipitates were subjected to Western blot analysis with anti-Myc and anti-FLAG antibodies (right panels). In (B), the CHC immunoprecipitates were examined for the presence of GAK, while (C) is the reciprocal experiment, where the GAK immunoprecipitates were examined for the presence of CHC fragments. Asterisks indicate nonspecific bands. Putative degradation products (#) are also indicated. An arrowhead (in B, lane 8) indicates F-CHC2 band that is partly overlapped with IgG band.

slowly-migrating bands and a weak band at 170 kDa (denoted by arrows). It also seems that the putative phosphorylated band of the doublet bands (large arrowhead) is detected primarily in the nucleus by the monoclonal antibodies. At least two additional bands (small arrowheads) were detected in both fractions but in larger amounts in the cytoplasmic fraction. These observations suggest that the cytoplasmic and nuclear GAK molecules are modified differently.

GFP-GAK localizes in both cytoplasm and nucleus

To examine which domain of GAK is required for its nuclear localization, we dissected GAK into two parts and fused them to green fluorescent protein (GFP) for *in vivo* visualization under a microscope (Fig. 2E). When we ectopically expressed the constructs in HeLa cells, we found that full length GAK was distributed primarily in the cytoplasm and sparsely in the nucleus (Fig. 2F). In contrast, the N-terminal construct bearing the kinase domain was observed exclusively in the cytoplasm while the C-terminal construct that lacked the kinase domain was found in both the cytoplasm and nucleus, although at a higher proportion in the nucleus than full length GAK. We confirmed by Western blot analysis that the transfected cells expressed intact GFP-GAK proteins of the expected size (Fig. 2G, arrows). These results indicate that the C-terminal part of GAK is required for its nuclear localization. Notably, the ectopically expressed GFP-GAK proteins failed to form dots in the nucleus, and were instead homogeneously distributed (Fig. 2F). This is probably because the ectopically expressed GFP-GAK escaped from modifications and failed to form a complex with its nuclear association partners. Indeed, the full size GFP-GAK protein, like the ectopically expressed full size Myc-GAK protein shown in modification, was observed upon Western blot analysis as a single band (Fig. 2G, see arrow in the leftmost lane) without any other slowly migrating bands. These putative modifications of GAK and their physiological significance will be more rigorously investigated in the future.

GAK complexes with cyclin G1, p53 and PP2A B′α in the nucleus

It is known that cyclin G1 forms a complex with PP2A B′ and p53 (Okamoto *et al.* 2002). To determine whether GAK is included in this complex, we first dissected GAK into four parts (Fig. 3A, left), tagged them with 6Myc, and examined their association with cyclin G1 *in vivo* in 293T cells expressing FLAG-tagged cyclin G1. For this, the 293T cell extracts were immunoprecipitated with anti-Myc antibody and the resulting GAK immunoprecipitates were subjected to Western blot analysis using anti-FLAG antibodies. As expected, Cyclin G1 co-immunoprecipitated with full length GAK (M-GAK; Fig. 3B, lane 4). Moreover, we found that cyclin G1 associates with the non-kinase domain (M-Δk; Fig. 3B, lane 6) but not the kinase domain (M-k; Fig. 3B, lane 8) of GAK. Reciprocal immunoprecipitation (Ip) using anti-FLAG antibody and Western analysis confirmed that cyclin G1 associates with M-GAK, M-Δj and M-Δk (Fig. 3C, lanes 4, 8 and 12), but not M-j and M-k (Fig. 3C, lanes 16 and 20) of GAK. The result indicates that cyclin G1 associates with the non-kinase domain of GAK.

We next examined whether GAK associates with p53 *in vivo*. For this, we co-transfected 293T cells with the 6Myc-GAK fragments described above. Immunoprecipitation of the GAK fragments and Western blotting with anti-p53 antibodies revealed that p53 does associate with almost full-length (see Fig. 3A) J-domain minus GAK (M-Δj), albeit weakly (Fig. 3D; arrowhead in lane 6). Moreover, we showed that the nonkinase domain (Δk) of GAK also associates rather strongly with p53 (Fig. 3D; arrowhead in lane 8). When we performed the reciprocal experiment using anti-p53 antibody as the immunoprecipitating antibody, only very weak GAK bands were detected for M-Δj alone (Fig. 3E, arrow in lane 9). That 6Myc-GAK binds rather strongly to p53 when anti-Myc antibody is used for immunoprecipitation but binds only weakly when anti-p53 antibody is used for immunoprecipitation suggests that only a small proportion of the p53 molecules in the cell bind to GAK *in vivo*. It was very difficult to show the interaction of these nuclear proteins including GAK, Cyclin G1, PP2A and p53 at endogenous level primarily due to the low sensitivity of the available antibodies.

Nuclear form of PP2A B′α subunit complexes with GAK

We next determined whether PP2A B′α1 (depicted in the left panel of Fig. 4A) associates with GAK by co-transfecting 293T cells with FLAG-tagged B′α1 and the 6Myc-GAK fragments described above. Note that B′α1, B′α2 and B′α3 are generated from the same gene by alternative splicing and only differ from each other in their C-terminal portions (Fig. 4A). Immunoprecipitation of the GAK fragments with anti-Myc antibody and Western blotting with anti-FLAG antibodies revealed that B′α1 binds to M-GAK, M-Δj, M-Δk and M-k (Fig. 4B, lanes 4, 6, 8 and 12) but not M-j alone (Fig. 4B, lane 10), unlike cyclin G1 and p53, which do not associate with

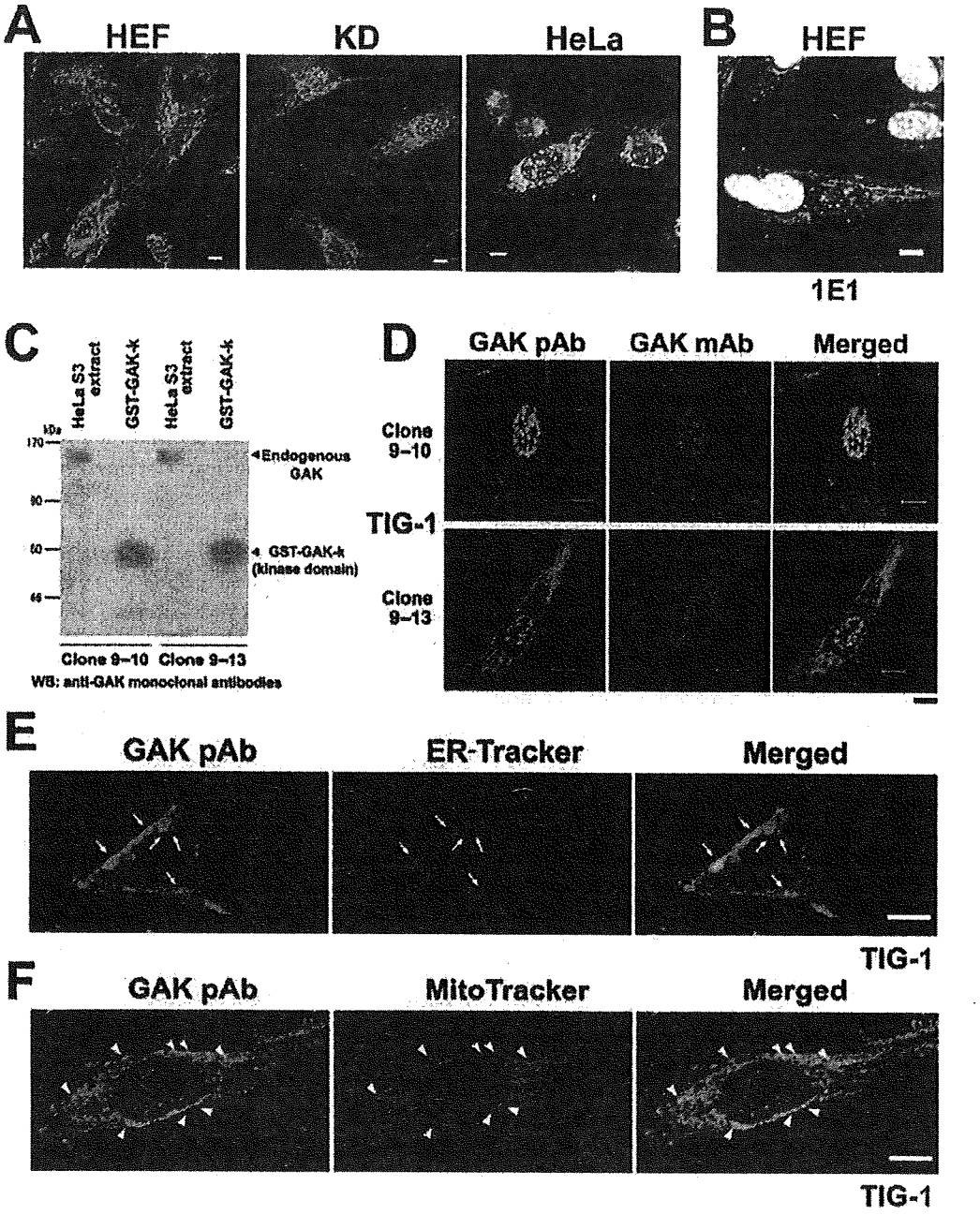

Figure 1 Subcellular localization of GAK, as detected by polyclonal and monoclonal antibodies. (A) Immunostaining of human GAK in HEF, KD and HeLa cells with the polyclonal anti-GAK antibody pGAK. (B) Immunostaining of HEF cells with the monoclonal anti-GAK antibody 1E1. (C) Western blot analysis of endogenous GAK in HeLa cell extract by using the monoclonal anti-GAK monoclonal antibodies 9–10 and 9–13. As a control, the purified GST-GAK (kinase domain) fusion protein was probed. (D) Immunostaining of TIG-1 cells with the monoclonal anti-GAK antibodies 9–10 and 9–13 (middle panels). As a control, the cells were stained with the pGAK polyclonal antibody (left panels). (E) Immunostaining of TIG-1 cells with pGAK polyclonal antibody and the ER staining marker ER-Tracker™ Red. Arrows indicate the colocalized regions. (F) Immunostaining of TIG-1 cells with pGAK polyclonal antibody and the mitochondrial staining marker MitoTracker™ Red. Arrowheads indicate the colocalized regions. Immunofluorescence micrographs were obtained by laser scanning microscope (Zeiss, LSM410 or LSM510) and dual color images were obtained and analyzed by co-localization image processing software. The merged images are shown in the right panels (D, E and F). Bars represent 10 μm.

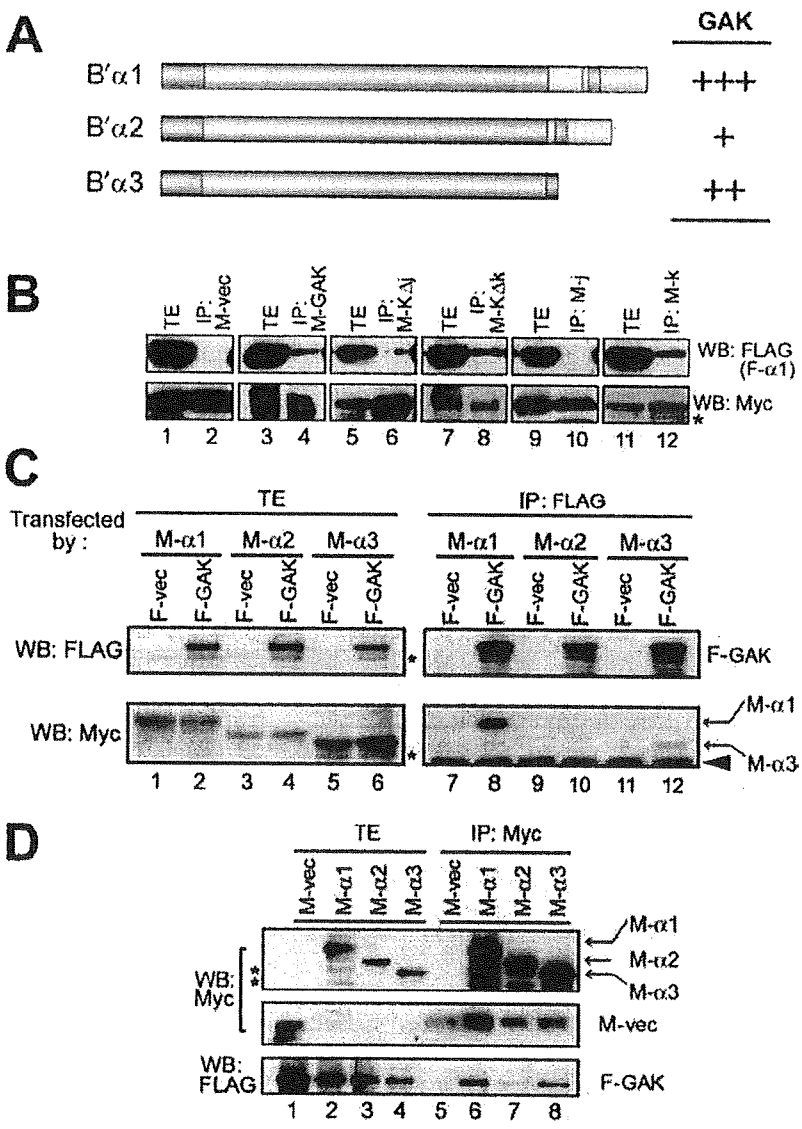

Figure 4 GAK associates with all three B'α (1–3) subtypes. (A) Schematic depiction of the PP2A B'α subtypes (left panels) and a summary of their ability to associate with GAK (right panel). Two or three pluses signify a stronger association. (B) Western blots to show that GAK associates with B'α1 via its kinase and non-kinase domains. 293T cells were co-transfected with 3FLAG-tagged B'α1 (F-α1) and various 6Myc-tagged GAK fragments, immunoprecipitated (IP) with anti-Myc antibody and subjected to Western blot analysis (WB) with anti-Myc and anti-FLAG antibodies. (C, D) Western blots to show that GAK associates most strongly with B'α1, weakly with B'α3, and very faintly with B'α2. 293T cells were co-transfected with FLAG-tagged full-length GAK and Myc-tagged B' isoforms and the total cell extract (TE) was directly subjected to Western blot analysis with anti-Myc and anti-FLAG antibodies (left panels). Alternatively, the extracts were immunoprecipitated (IP) with anti-FLAG antibody (C) or anti-Myc antibody (D) and the immunoprecipitates were subjected to Western blot analysis with anti-Myc and anti-FLAG antibodies (right panels). Asterisks indicate non-specific bands. Arrowhead in (C) indicates a band for IgG used for immunoprecipitation that served as a loading control.

GAK associates with CHC in the nucleus

Because GAK regulates the uncoating of clathrin-coated vesicles (Eisenberg & Greene 2007), it is likely that GAK associates with CHC directly. To gain insights into this interaction, we dissected CHC into five parts according to Edeling *et al.* (2006) and N-terminally FLAG-tagged them (Fig. 5A, denoted as CHC1~5 in left panel). Because the CHC5 fragment was too small to be detected by FLAG-tagging, we tagged it with Myc instead. 293T cells were co-transformed with each CHC fragment and full-length GAK reciprocally tagged with Myc or FLAG (M-GAK or F-GAK, respectively). The CHC fragments were then immunoprecipitated with anti-FLAG antibody (CHC1~4) or anti-Myc antibody (CHC5) and subjected to Western blot analysis using either antibody. This revealed that GAK associates strongly with CHC1, 2 (Fig. 5B-i, lanes 6 and 7), 4 (Fig. 5B-ii, lane 4) and 5 (Fig. 5B-iii, lane 4) but only weakly with CHC3 (Fig. 5B-i, lane 8). This was confirmed by reciprocal immunoprecipitation of GAK and Western analysis of the CHC fragments contained in these immunoprecipitates as follows: CHC1 (Fig. 5C-i, lane 4), CHC2 (Fig. 5C-ii, lane 4), CHC3 (Fig. 5C-iii, lane 4), CHC4 (Fig. 5C-iv, lane 4) and CHC5 (Fig. 5C-v, lane 4).

which is the nuclear form of B′α. Finally, immunostaining revealed the nuclear signals, but not the cytoplasmic signals, of B′α colocalized with GAK (Fig. 7A, see merged image and right panel). PP2A is now considered to be a tumor suppressor because inactivation of PP2A by viral oncoproteins, mutation of specific subunits, or overexpression of endogenous inhibitors contributes to cell transformation by regulating specific phosphorylation events (reviewed in Westermarck & Hahn 2008). Indeed, we previously found a truncated mutation of B′α subunit (ΔB′α) in highly metastatic mouse melanoma BL6 cells (Ito *et al.* 2000). This ΔB′α variant lacks N-terminal 65 amino acids due to retrotransposon insertion and its endogenous overexpression enhanced cell motility through hyper-phosphorylation of paxillin. Moreover, overexpression of ΔB′α also damaged the cell cycle checkpoint and enhanced the genetic instability of tumors, which promotes tumor progression from the nonmetastatic to the metastatic state (Ito *et al.* 2003). Thus, B′α, in collaboration with GAK, may also be involved in tumor progression.

GAK was recently reported to be an AR-interacting transcriptional coactivator (Ray *et al.* 2006). Given that the signal transduction pathway that leads to AR activity is also regulated by the phosphorylation and dephosphorylation of particular proteins, it is possible that GAK is also involved in this hormone signaling pathway. It should be remembered here that transcription occurs in the nucleus. Because GAK was first identified as an AR-interacting protein by using the Tup1-repressed transactivator system, it is possible that GAK will also be detected in other transcriptional complexes. This is supported by the recent report of Enari *et al.* (2006) mentioned above, which suggests that GAK also acts as a transcriptional coactivator in collaboration with CHC. We also showed that B′α is concentrated in intranuclear structures known as nuclear speckles (Fig. 7A) that are macromolecular structures that accumulate transcription and splicing factors in cardiomyocytes (Gigena *et al.* 2005). It remains to be determined by our future experiments whether any GAK-mediated events are actually involved in these transcription regulatory events.

Experimental procedures

Cell culture

The HEF line is a gift from Dr M. Yutsudo. HeLa cells were provided by the Japanese Cancer Research Resources Bank (JCRB). The other human cells that were used were purchased from the American Type Culture Collection. The cells were maintained in 5% CO_2 at 35 °C in Dulbecco's modified Eagle's medium (DMEM) supplemented with 5% fetal bovine serum (Hyclone Laboratory, Logan, UT), penicillin (100 U/mL), and streptomycin (100 μg/mL).

Antibodies

Anti-GAK monoclonal antibodies were produced in our laboratory by immunizing mice with rat GST-GAK fusion protein according to standard methods. The monoclonal antibodies that recognized GST were excluded during screening. Polyclonal antibodies against rat GAK, human cyclin G1 or Orc2 were generated by immunizing New Zealand White rabbits with GST-rat GAK, GST-human cyclin G1 or GST-human Orc2 via standard techniques. Antibodies that recognized the GST portion were removed by affinity chromatography using GST-bound resin. An anti-PP2A-B′α polyclonal antibody that does not distinguish between the B′α1, -2 or -3 subtypes was prepared as reported previously (Ito *et al.* 2000). Antibodies against the following antigens were purchased: Myc (Oncogene Science, Uniondale, NY), actin, GFP (MBL, Nagoya, Japan), p53 (DO-1; Santa Crutz Biotechnology, Santa Cruz, CA), CHC (BD bioscience, San Jose, CA), GAPDH (Fitzgerald Industries International, Inc., Concord, MA) and FLAG (Zymed, San Francisco, CA).

Fluoroimmunostaining

Cells (synchronized or in log phase) were cultured on coverslips immersed in a culture dish (ϕ = 6 cm) and fixed by sequential 10 min treatments at 20 °C with 3.7% formamide, 0.1% Triton X-100, and 0.05% Tween 20 in PBS. After removing the medium, the cells on coverslips were rinsed for 5 min three times with 2 mL TBST buffer (20 mM Tris-HCl [pH 7.5], 150 mM NaCl, 0.05% Tween 20) supplemented with 2% bovine serum albumin (BSA; Sigma) at room temperature. Subsequently, 100 μL of TBST containing the relevant antibody was spotted on parafilm and the coverslips were lifted and laid cell-side down on the liquid. After incubation at room temperature for 1 h, the coverslips were rinsed in culture dishes cell-side up with TBST/BSA as described above. FITC- or Texas Red-linked anti-rabbit Ig (from donkey; Amersham) or Texas Red-linked anti-mouse Ig (from sheep; Amersham) served as secondary probes and were incubated with the cells attached to the coverslips for 1 h and rinsed three times as described above. MitoTracker™ Red and ER-Tracker™ Red was purchased from Molecular Probes (Invitrogen) Inc. (Eugene, OR). Photographs were taken and the images were recorded by a inverted laser scan microscope (Zeiss LSM410 or LSM510).

Immunoprecipitation and Western blot analysis

Immunoprecipitation was performed essentially as described previously (Kanaoka *et al.* 1997). Briefly, cells were collected and lysed in lysis buffer (50 mM Tris-HCl [pH 7.5], 250 mM NaCl, 0.1% Nonidet P-40) supplemented with protease inhibitors (2 μg/mL aprotinin, 2 μg/mL of leupeptin, 1 μg/mL pepstatin A, 50 μg/mL PMSF, 1 mM EGTA). After clarifying the extract by centrifugation at 10 000 × *g* for 5 min; aliquots of the supernatant

CHC associates with GAK via a different domain in the nucleus

To examine if this association pattern differs between the cytoplasm and nucleus, we fractionated the cell extracts as described above (see Fig. 2D) and performed Ip/Western analyses similar to those described above in relation to Fig. 5. We found that GAK predominantly associated with the CHC1 and 5 fragments in the nucleus (Fig. 6A) but in the cytoplasm predominantly associated with CHC2 and 4. Again, we found negligible association between GAK and the CHC3 fragment in either compartment. Successful fractionation was confirmed by subjecting the fractionated extracts to Western blot analysis using anti-Orc2 (nuclear control), anti-α tubulin (cytoplasmic control) antibodies (Fig. 6B). These observations together suggest that CHC associates with GAK via a different domain depending on whether it is in the nucleus or cytoplasm as schematically depicted in Fig. 6C (see Discussion). This in turn suggests that the nuclear function(s) of GAK and clathrin differs from their role in cytoplasmic vesicle trafficking (see Discussion). The ability of GAK to associate with each of the CHC fragments is summarized in the right panel of Fig. 5A (right panel).

Subcellular colocalization of GAK with nuclear proteins

To investigate where in the cell the biochemical associations between GAK and PP2A B′α, cyclin G1, p53, and CHC occur, we subjected TIG-1 cells to immunohistochemical analysis using specific antibodies against each protein. When we examined whether GAK colocalized with PP2A B′α, we found that B′α also displayed strong nuclear dots, and that about 25% of these merged with the nuclear GAK signals (yellow; Fig. 7A). In contrast, the cytoplasmic signals colocalized poorly. Although the anti-B′α antibody cannot distinguish between the different subtypes (Ito *et al.* 2000), we concluded that it was predominantly the B′α1 isoform that colocalizes with GAK as nuclear dots given that B′α1 and B′α2, but not B′α3, localize in the nucleus and that GAK associates more strongly with B′α1 than with B′α2 (Fig. 4). Cyclin G1 is known to show marked immunostaining in the nucleus and sparse staining throughout the cytoplasm (Reimer *et al.* 1999). Indeed, about 20% and 30% of the cyclin G1 and p53 signals colocalized with GAK, respectively (Fig. 7B,C). These results suggest that about 20~30% of B′α1, cyclin G1 and p53 complex with nuclear GAK.

Most of the CHC signals were detected in the cytoplasm and very few of these merged with the GAK signals (Fig. 7D, upper panels). However, CHC also displayed dots in the nucleus. This was observed only when the CHC signal was highlighted because the nuclear CHC signals represent only about 5% of the cytoplasmic CHC signals (Enari *et al.* 2006). Surprisingly, almost all nuclear CHC dots colocalized with GAK (Fig. 7D, lower panels), which suggests that most of the nuclear CHC functions together with GAK.

Discussion

The ubiquitously expressed GAK protein is known to regulate endocytosis in the cytoplasm (Eisenberg & Greene 2007). In the present study, we showed that GAK localizes not only in the cytoplasm but also in the nucleus. This nuclear localization of GAK was confirmed by immunostaining HeLa, HEF, KD and TIG-1 cells using both polyclonal and monoclonal antibodies specific for the GAK protein (Fig. 1A,B,D), performing Western blotting with anti-GAK antibodies on the nuclear and cytoplasmic fractions of 293T cells (Fig. 2D), and observing GFP-GAK in transfected HeLa cells under a microscope (Fig. 2E–F). That the 9–10 monoclonal antibody only recognized the nuclear form of GAK while the 9–13 monoclonal antibody recognized both cytoplasmic and nuclear GAK suggests that nuclear GAK bears an epitope that is not present in cytoplasmic GAK. This in turn suggests GAK is modified somehow in either the cytoplasm or nucleus. Indeed, we found that nuclear GAK is phosphorylated (Fig. 2A–D), although we cannot yet exclude the possibility that cytoplasmic GAK is also phosphorylated (Fig. 2D). We also showed that this phosphorylation event was mediated by another, as yet unknown protein kinase rather than by self-activity because GAK-KD was phosphorylated to the same degree as wild-type GAK (Fig. 2B,C). The identification of this kinase will be the subject of our future study. The nuclear localization of GAK was independent of p53 activity because it was observed in both HEF, KD (Fig. 1A) and TIG-1 (Fig. 7) cells which harbor wild type p53, in HeLa cells (Fig. 1A) which lack p53, and in 293T cells (Fig. 6), in which p53 is present but is inactivated by large T antigen, a major early gene product encoded by SV40 (Lilyestrom *et al.* 2006). The results presented here thus indicate that GAK is not only important in the cytoplasm as a regulator of vesicle trafficking, but it also plays an important role in the nucleus.

Like its cytoplasmic function in vesicle trafficking, one of the nuclear functions of GAK may also relate to CHC since we showed that CHC is also present in the nucleus, albeit at much lower levels than in the cytoplasm (Fig. 7D). This nuclear localization of CHC was also reported by

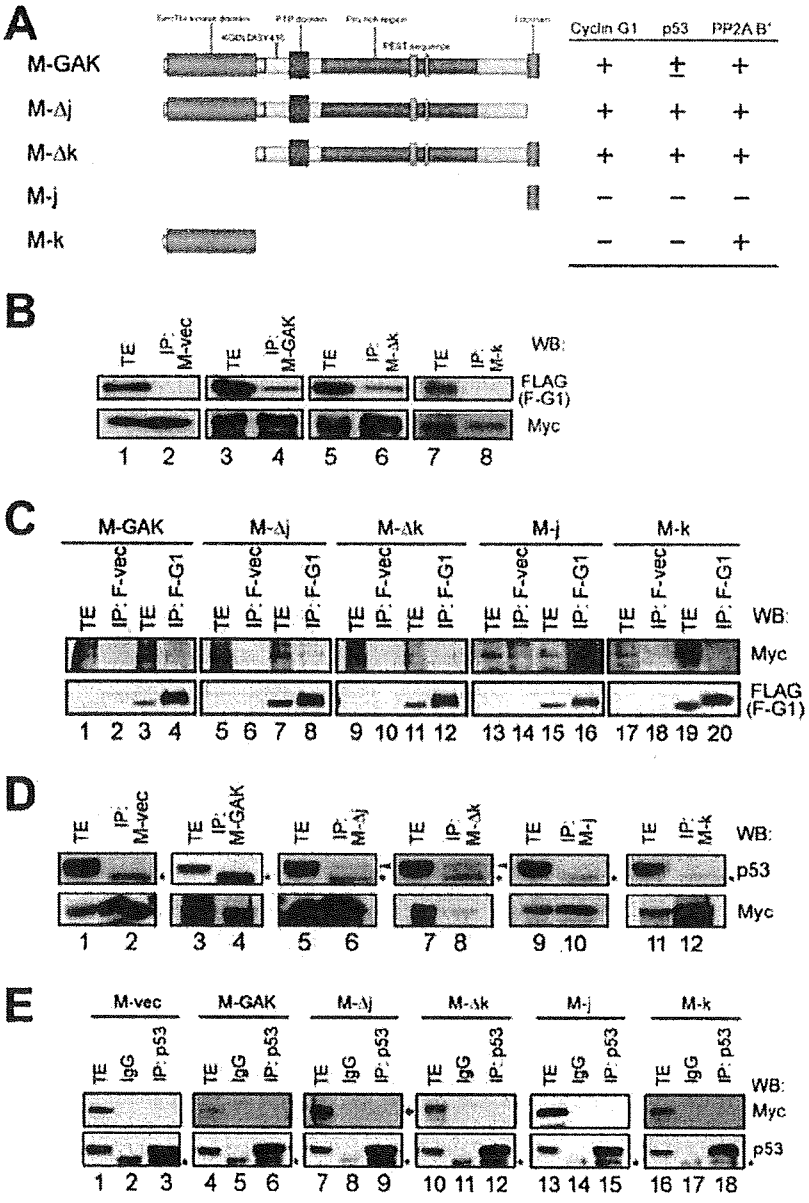

Figure 3 GAK associates *in vivo* with the nuclear proteins cyclin G1 and p53. (A) Schematic depiction of the GAK fragments (left panel) and a summary of their ability to associate with cyclin G1, p53, and B'α (right panel). Colored domains are kinase domain (orange), linker domain (yellow), PTP domain (purple), Proline rich region (blue), PEST sequence (light blue), C-terminal region (green) and J domain (red). Minus, no association; plus/minus, weak association; plus, association. (B, C) GAK associates with cyclin G1 via its non-kinase domain. 293T cells were transfected with FLAG-cyclin G1 and various 6-Myc-tagged GAK fragments. The 6-Myc-tagged GAK fragments used in this study are depicted in Fig. 2A and include full length GAK (M-GAK), GAK lacking the J domain (M-ΔJ), GAK lacking the kinase domain (M-Δk), the J domain of GAK (M-J) and the GAK kinase domain (M-k). As controls, empty 6Myc-expressing (M-vec) and FLAG-expressing (F-vec) vectors were used. The cell extracts were immunoprecipitated (IP) with anti-Myc antibody and the immunoprecipitates were subjected to Western blot analysis with the same antibodies. F-G1, the anti-FLAG-cyclin G1 antibody. (D, E) GAK associates weakly with p53 via its non-kinase domain. 293T cells expressing 6Myc-tagged GAK fragments and endogenous p53 were immunoprecipitated with anti-Myc (D) or anti-p53 (E) antibodies and subjected to Western blotting with the same antibodies. Asterisks indicate nonspecific bands. TE, total cell extract. IgG, a non-immune IgG control for the p53 antibody.

the kinase domain of GAK (Fig. 3). The ability of cyclin G1, p53 and B'α1 to associate with the various GAK fragments are summarized in the right panel of Fig. 3A.

We previously showed that B'α1 and B'α2, but not B'α3, localize predominantly in the nucleus (Ito *et al.* 2000). Thus, we next asked which B'α subtype preferentially associates with GAK. For this purpose, we co-transformed 293T cells with FLAG-tagged full-length GAK and N-terminally Myc-tagged B'α1, B'α2 or B'α3. Immunoprecipitation of GAK and Western blot analysis of the immunoprecipitates using anti-Myc antibodies revealed that GAK associated most strongly with B'α1 and recognized B'α2 and B'α3 very faintly and weakly, respectively (Fig. 4C, lanes 8, 10 and 12). This was confirmed by reciprocal immunoprecipitation/Western blot analysis (Fig. 4D, lanes 6, 7 and 8). It was very difficult to show the interaction of these nuclear proteins at the endogenous level because of low sensitivity of our antibodies. To cover this problem, we performed IP/Western analysis under over expression condition.

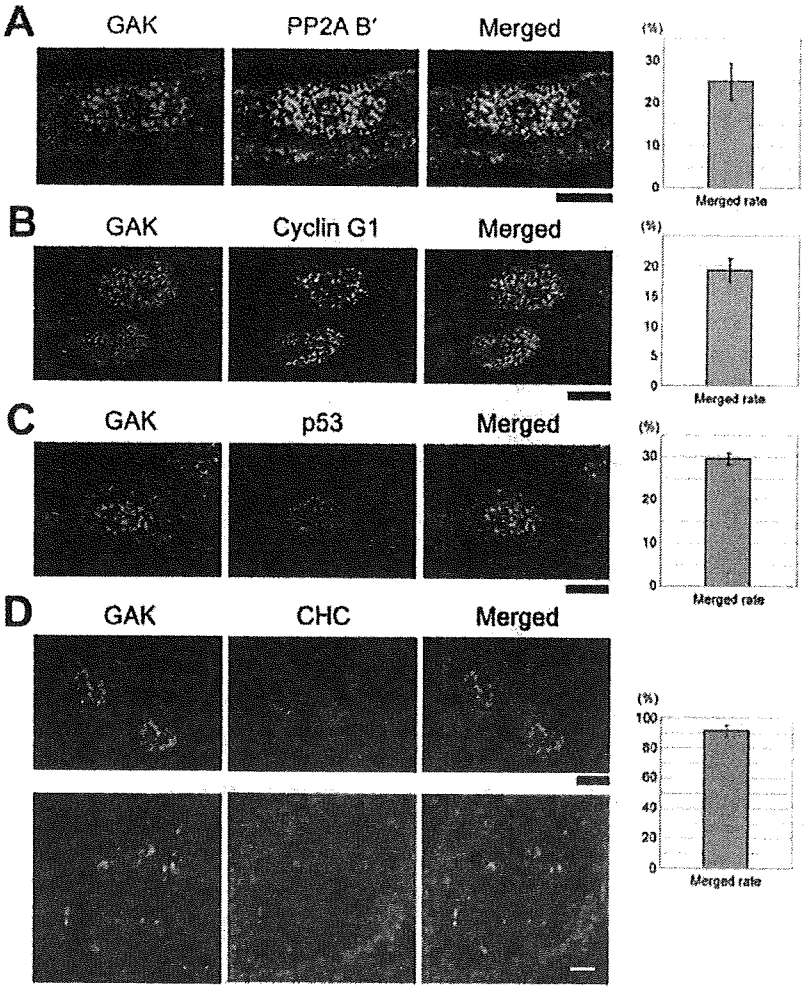

Figure 7 Nuclear co-localization of GAK with its association partners. TIG-1 cells were immunostained with the 9–13 anti-GAK monoclonal antibody (A, B) or pGAK polyclonal antibody (C, D) together with antibodies against PP2A B′α (A), cyclin G1 (B), p53 (C) or CHC (D). The bar graphs show the percentages of yellow signals relative to the total number of nuclear PP2A/cyclin G1/p53/CHC signals in the merged images. The standard deviations in the graph were calculated from 10 cells for PP2A B′α and 3 cells for each of the others. Black bars = 10 μm. White bar = 2 μm.

Enari *et al.* (2006). Moreover, we found that nearly all of the nuclear CHC molecules associated with GAK (Fig. 7D, see merged image). Notably, the portion of CHC that associates with GAK differs depending on whether the two proteins occur in the cytoplasm or the nucleus (Fig. 6A). Thus, while GAK associates with the middle part of CHC (CHC2 and CHC4) in the cytoplasm, it interacts with its N- and C-termini (CHC1 and CHC5) in the nucleus (Fig. 6C). The binding of GAK to the termini of CHC means that the CHC junction is occupied by GAK (see Fig. 5), which is likely to prohibit the formation of clathrin-coated vesicles in the nucleus. Moreover, it may also affect the interaction between p53 and CHC because p53 associates with the C-terminus of CHC (Enari *et al.* 2006). This explains why GAK only colocalized with CHC in the nucleus (Fig. 7D). Notably, it was recently reported that the p53-binding site of CHC behaved as a monomer in cells and had a higher ability to transactivate p53 (Ohmori *et al.* 2008). Thus, it is likely that CHC adopts a distinct conformation in the nucleus (e.g. as a single triskelion or fibrous structure). These observations together with our own suggest that GAK and CHC may collaborate not only in the cytoplasm as vesicle transporters but also in the nucleus as regulators of p53-mediated transcription.

Another apparent nuclear function of GAK is to regulate the activity of B′α1 when it is recruited by cyclin G1 to its dephosphorylation target proteins (Okamoto *et al.* 1996). This is shown by the following observations. First, GAK preferentially complexes with cyclin G1 (Fig. 3), which is shown to be predominantly localized in the nucleus (Fig. 7B). Second, B′α1 localized in the nucleus, although the anti-PP2A B′α antibody we used here also recognized B′α3 subunit that is present in the cytoplasm as well (Fig. 7A). Third, Ip/Western analysis indicated that GAK bound preferentially to B′α1 (Fig. 4),

Pathology

Pathology International 2009; **60**: 112–118 doi:10.1111/j.1440-1827.2009.02484.x

Case Report

Repeated stent thrombosis after DES implantation and localized hypersensitivity to a stent implanted in the distal portion of a coronary aneurysm thought to be a sequela of Kawasaki disease: Autopsy report

Yuki Yokouchi,[1] Toshiaki Oharaseki,[1] Fumie Ihara,[1] Shiro Naoe,[2] Shigetada Sugawara[3] and Kei Takahashi[1]

[1]Department of Surgical Pathology, Toho University Ohashi Medical Center, Tokyo, [2]Department of Biomedical Engineering, Toin University of Yokohama and [3]Division of Cardiology, Yokohama General Hospital, Kanagawa, Japan

The patient was a 40-year-old Japanese woman. At 37 years of age she underwent stent implantation in LAD#7 for an acute myocardial infarction. Subsequently, coronary intervention was performed four times because of occlusion of the stent. Sudden death occurred at 40 years of age due to ventricular tachycardia. Clinically, the patient had had no history of collagen disease, anti-phospholipid antibody syndrome or coagulation disorder. The autopsy revealed only very mild atherosclerotic changes in the aorta and various other organs, but concentric thickening of the intima was observed in all three branches of the coronary arteries. Also, aneurysms accompanied by calcification were observed at each of LAD #6, LCx #11 and RCA #4PD. The stent was occluded with a thrombus, and the vascular walls showed infiltration by lymphocytes, plasma cells and numerous eosinophils. The eosinophil infiltration was confined to the site of the stent. It was surmised that the patient had experienced late stent thrombosis due to a hypersensitivity reaction to the DES on the basis of a development of a state of high susceptibility to thrombus formation because of a coronary aneurysm. The aneurysm was suspected of being a post-inflammatory change of Kawasaki disease.

Key words: eosinophils, hypersensitivity reaction, Kawasaki disease, pathology, stent thrombosis

Stent thrombosis (ST) is known to occur regardless of whether a conventional bare-metal stent (BMS) or a drug-eluting stent (DES) is implanted. The prognosis is poor in such cases, and ST can be an important cause of death after stent implantation. It is said that the incidence of ST is 1% or less if antiplatelet therapy using aspirin or ticlopidine is administered.[1] Most ST events occur within one week after stent implantation, but it has been reported that the incidence of late stent thrombosis (LST), occurring 30 or more days after stent implantation, is 0.23% when using a BMS and 0.25–1.4% when using a DES.[2,3] One possible cause of ST is manifestation of a hypersensitivity reaction in relation to the stent, but there have been few published reports demonstrating involvement of such a hypersensitivity reaction on the basis of histopathological findings.

We performed an autopsy on a young Japanese woman who had repeatedly developed ST. The histopathological findings showed multiple coronary artery aneurysms, which we surmised to be residual lesions derived from the coronary arteritis of Kawasaki disease. Moreover, those findings led us to conclude that a hypersensitivity reaction to a stent implanted distal to a coronary aneurysm was one of the causes of the ST.

CASE REPORT

Clinical summary

The patient was a 40-year-old Japanese woman. Her only coronary risk factor was smoking (20 cigarettes/day for 20 years). She first experienced acute myocardial infarction at 37 years of age. Coronary angiography showed total occlusion of LAD #7, 75% stenosis proximal to LCx #11, and total occlusion of RCA #4PD. In addition, coronary artery aneurysms had formed at LCx #11 and RCA #4PD (Fig. 1a–c). A ectatic lesion at LAD #6 was also noted at that time. A

Correspondence: Yuki Yokouchi, MD, Department of Surgical Pathology, Toho University Ohashi Medical Center, 2-17-6, Ohashi, Meguro-ku, Tokyo, 153-8515, Japan. Email: tyuki@med.toho-u.ac.jp

Received 1 December 2008. Accepted for publication 29 September 2009.

were first immunoprecipitated by using protein A-Sepharose alone. The clarified lysates were subsequently immunoprecipitated by using the relevant antibodies. Thereafter, equal quantities of fresh or immunoprecipitated cell extract were adsorbed to protein A-Sepharose, pelleted and subjected to 10% SDS-polyacrylamide gel electrophoresis (SDS-PAGE). For Western blotting, total cellular proteins and immunoprecipitates resolved on gels were transferred to nitrocellulose filters and probed with the relevant antibodies. Immunoreactive protein bands were visualized by using Renaissance™ chemiluminescence reagents (DuPont NEN, Boston, MA).

Preparation of GFP-, GST-, FLAG- or Myc-fusion constructs

To fuse genes in-frame to GFP (green fluorescent protein), a synthetic linker was inserted into the pEGFP-C1 vector (Clontech, Palo Alto, CA); this linker was designed to allow cDNA inserts to be inserted in-frame via *AscI-NotI* sites. To obtain cDNA inserts for human GAK carrying in-frame *AscI-NotI* sites, oligonucleotides with sequences around the initiation codon and the termination codon that contained an *AscI* site and a *NotI* site, respectively, were synthesized and used as PCR primers for PCR with the relevant cDNA substrate. The identity of each gene was confirmed by DNA sequencing of four independent clones, and the plasmid DNA without a mismatched DNA sequence was selected and cut with *AscI* and *NotI*. The resulting cDNA inserts were incorporated into the GFP-vectors.

A similar strategy was used to create other plasmid constructs that express GST, FLAG or Myc-fusion proteins. The primer pairs used for PCR amplification during the process of these manipulations are listed in Supplementary Table S1. All plasmid constructs were transfected into HeLa or 293T cells by using *Trans*IT™ polyamine transfection reagents (Pan Vera Corporation, Madison, WI) according to the manufacturer's protocol. The expressed GFP-fusion proteins were visualized by using a Zeiss LSM510 confocal photomicroscope.

Acknowledgements

We are obliged to Dr Takahiro Nagase (Kazusa DNA Research Institute, Japan) for the CHC plasmid (KIAA0034) and Dr M. Yutsudo (RIMD, Osaka University) for the gift of HEF cells. We thank Dr P. Hughes for critically reading the manuscript. This work was supported in part by Innovation Plaza Osaka of the Japan Science and Technology Agency (JST), and by grants-in-aid for Scientific Research on Priority Areas 'Applied Genomics', Scientific Research (S), Exploratory Research, and the Science and Technology Incubation Program in Advanced Regions, from the Ministry of Education, Culture, Sports, Science and Technology of Japan to Hiroshi Nojima.

References

Bernardi, R. & Pandolfi, P.P. (2007) Structure, dynamics and functions of promyelocytic leukaemia nuclear bodies. *Nat. Rev. Mol. Cell Biol.* **8**, 1006–1016.

Biamonti, G. (2004) Nuclear stress bodies: a heterochromatin affair? *Nat. Rev. Mol. Cell Biol.* **5**, 493–498.

Chen, X. (2002) Cyclin G: a regulator of the p53-Mdm2 network. *Dev. Cell* **2**, 518–519.

Chiodi, I., Corioni, M., Giordano, M., Valgardsdottir, R., Ghigna, C., Cobianchi, F., Xu, R.M., Riva, S. & Biamonti, G. (2004) RNA recognition motif 2 directs the recruitment of SF2/ASF to nuclear stress bodies. *Nucleic Acids Res.* **32**, 4127–4136.

Crockett, D.K., Lin, Z., Elenitoba-Johnson, K.S. & Lim, M.S. (2004) Identification of NPM-ALK interacting proteins by tandem mass spectrometry. *Oncogene* **23**, 2617–2629.

Edeling, M.A., Smith, C. & Owen, D. (2006) Life of a clathrin coat: insights from clathrin and AP structures. *Nat. Rev. Mol. Cell Biol.* **7**, 32–44.

Eisenberg, E. & Greene, L.E. (2007) Multiple roles of auxilin and hsc70 in clathrin-mediated endocytosis. *Traffic* **8**, 640–646.

Enari, M., Ohmori, K., Kitabayashi, I. & Taya, Y. (2006) Requirement of clathrin heavy chain for p53-mediated transcription. *Genes Dev.* **20**, 1087–1099.

Gigena, M.S., Ito, A., Nojima, H. & Rogers, T.B. (2005) A B56 regulatory subunit of protein phosphatase 2A localizes to nuclear speckles in cardiomyocytes. *Am. J. Physiol. Heart Circ. Physiol.* **289**, H285–H294.

Greener, T., Zhao, X., Nojima, H., Eisenberg, E. & Greene, L.E. (2000) Role of cyclin G-associated kinase in uncoating clathrin-coated vesicles from non-neuronal cells. *J. Biol. Chem.* **275**, 1365–1370.

Ito, A., Kataoka, T.R., Watanabe, M., Nishiyama, K., Mazaki, Y., Sabe, H., Kitamura, Y. & Nojima, H. (2000) A truncated isoform of the PP2A B56 subunit promotes cell motility through paxillin phosphorylation. *EMBO J.* **19**, 562–571.

Ito, A., Koma, Y., Watabe, K., Nagano, T., Endo, Y., Nojima, H. & Kitamura, Y.A. (2003) A truncated isoform of the protein phosphatase 2A B56gamma regulatory subunit may promote genetic instability and cause tumor progression. *Am. J. Pathol.* **162**, 81–91.

Janssens, V., Goris, J. & Van Hoof, C. (2005) PP2A: the expected tumor suppressor. *Curr. Opin. Genet. Dev.* **15**, 34–41.

Kametaka, S., Moriyama, K., Burgos, P.V., Eisenberg, E., Greene, L.E., Mattera, R. & Bonifacino, J.S. (2007) Canonical interaction of cyclin G associated kinase with adaptor protein 1 regulates lysosomal enzyme sorting. *Mol. Biol. Cell* **18**, 2991–3001.

Kanaoka, Y., Kimura, S.H., Okazaki, I., Ikeda, M. & Nojima, H. (1997) GAK: a cyclin G associated kinase contains a tensin/auxilin-like domain. *FEBS Lett.* **402**, 73–80.

Kimura, S.H., Ikawa, M., Ito, A., Okabe, M. & Nojima, H. (2001) Cyclin G1 is involved in G2/M arrest in response to DNA damage and in growth control after damage recovery. *Oncogene* **20**, 3290–3300.

Kimura, S.H. & Nojima, H. (2002) Cyclin G1 associates with MDM2 and regulates accumulation and degradation of p53 protein. *Genes Cells* **7**, 869–880.

Korolchuk, V.I. & Banting, G. (2002) CK2 and GAK/auxilin2 are major protein kinases in clathrin-coated vesicles. *Traffic* **3**, 428–439.

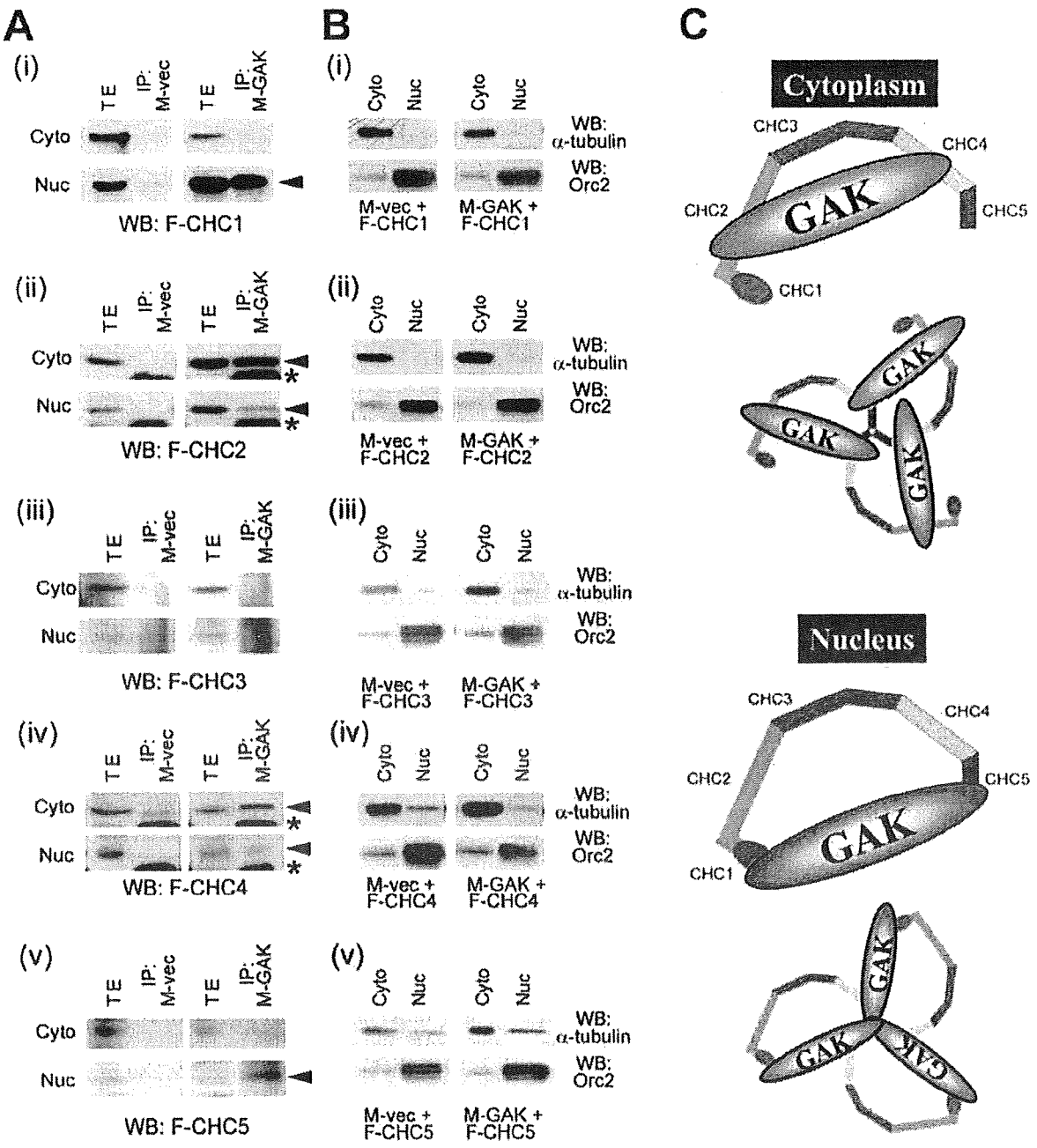

Figure 6 CHC associates with GAK via a different domain depending on whether it is in the cytoplasm or nucleus. 293T cells were co-transfected with CHC fragments and GAK and their lysates were biochemically separated into cytoplasmic and nuclear fractions. (A) The two fractions were directly subjected to Western blot analysis with anti-Myc and anti-FLAG antibodies (left panels). Alternatively, the extracts were immunoprecipitated (IP) with anti-Myc antibody and the immunoprecipitates were subjected to Western blot analysis with both antibodies to determine the presence of FLAG-CHC fragments in the Myc-GAK immunoprecipitates (right panels). Arrowheads and asterisks indicate the CHC fragment bands and nonspecific bands, respectively. (B) As controls, the fractions were subjected to Western blot analysis using anti-Orc2 (nuclear control), anti-α tubulin (cytoplasmic control) antibodies. Cyto, cytoplasmic fraction; Nuc, nuclear fraction. (C) Schematic depiction to show how CHC associates with GAK via a different domain in the cytoplasm or nucleus. Possible interactions of a single GAK molecule to CHC (upper panels), and three GAK molecules to CHC triskelion (lower panels) are shown (see Discussion for details).

Figure S1. Sato *et al.*

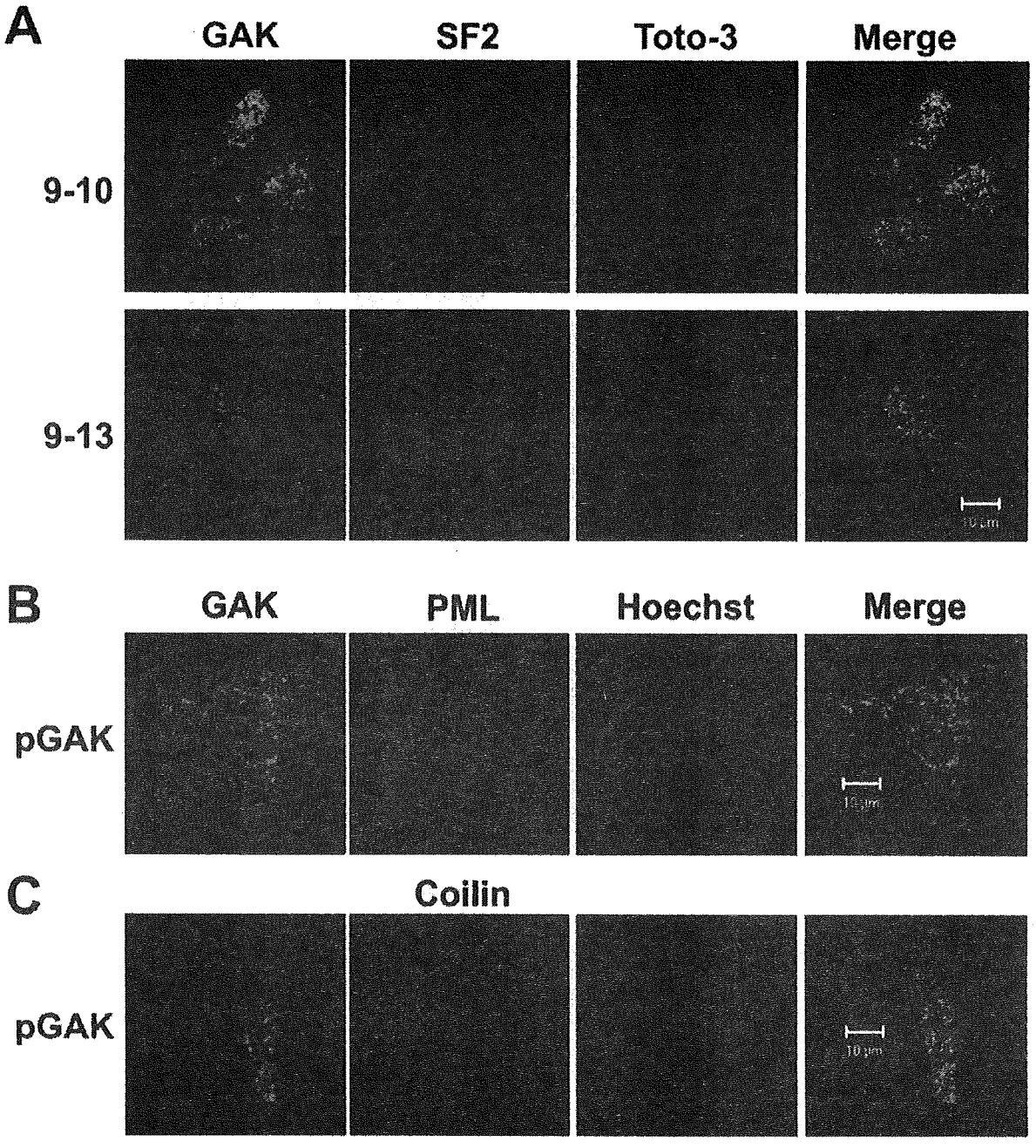

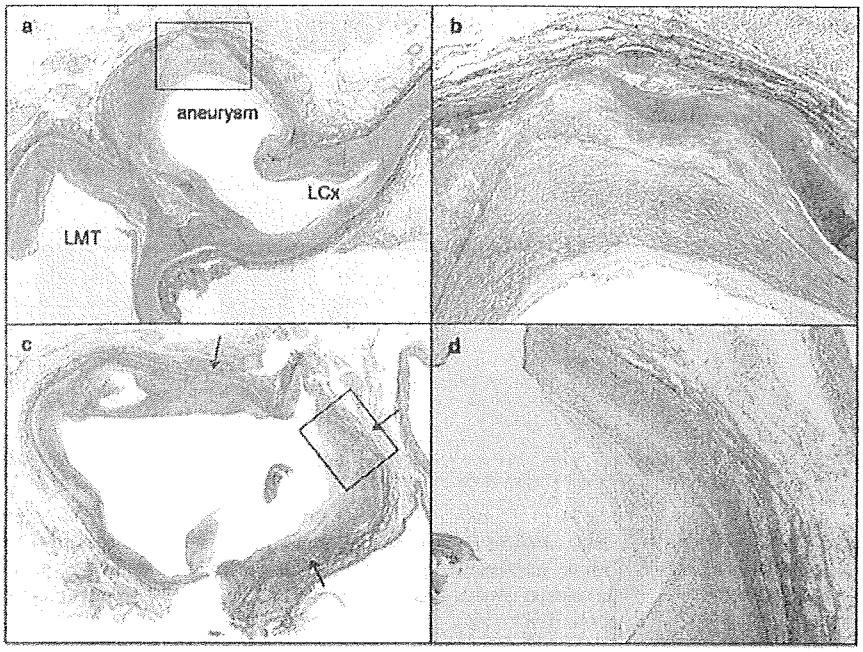

Figure 4 (a,b). Photomicrograph of coronary aneurysm that formed at LCx #11 (the site shown in Fig. 3-i). Destruction of the arterial architecture was completely destructed, that is, fibrous intimal thickening with lamellar calcification, disappearance of the internal elastic lamina and tunica media are seen. (**c,d**) Coronary aneurysm that formed at LAD #6, just proximal to the stent (the site shown in Fig. 3-ii). Fibrotic intimal thickening with focal calcification, extension and disruption of the internal elastic lamina and thinning of the tunica media are observed in the aneurysm wall. In addition, partial destructions of the internal elastic lamina and tunica media that might be caused by POBA also existed on the aneurysm wall (arrow). (EvG stain).

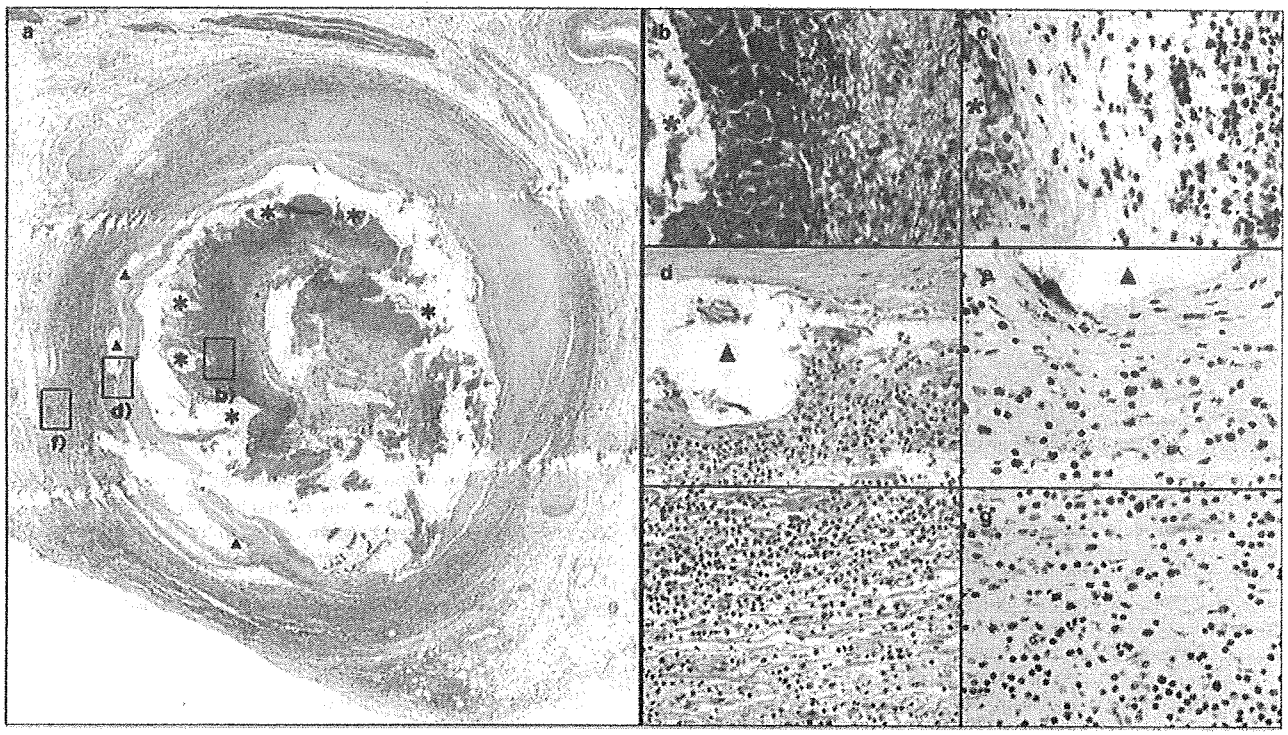

Figure 5 Photomicrograph of cross-sections of LAD #7 with implanted BMS and first DES (the site shown in Fig. 3-iii). (**a**) The lumen is occluded with a fibrin thrombus, and extensive infiltration by inflammatory cells is seen in the thrombus and all layers of the vascular wall. (HE stain). (**b,c**) The inflammatory cells are predominantly eosinophils in the thrombus around the DES stent strut (asterisk). (b: HE stain; c: Luna stain). (**d,e**) Environs of the BMS stent strut (arrow head). Many infiltrating eosinophils are seen. (d: HE stain; e: Luna stain). (**f,g**) Many eosinophils, in addition to plasma cells and lymphocytes, are seen to be infiltrating the adventitia. (f: HE stain; g: Luna stain).

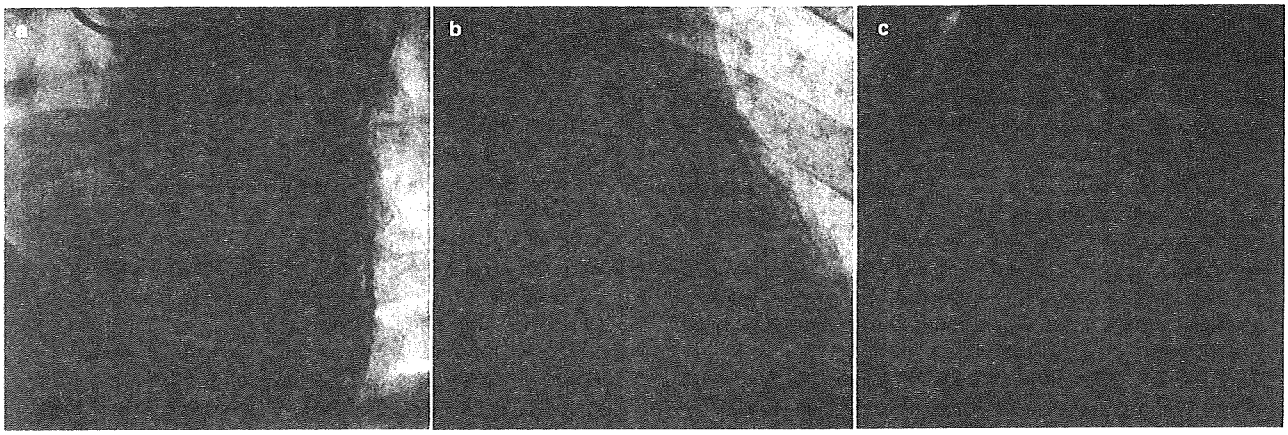

Figure 1 Coronary angiography administered at the first myocardial infarction shows total occlusion of LAD #7 (**a**), 75% stenosis proximal to LCx #11 (**b**) and total occlusion of RCA #4PD (**c**). In addition, coronary aneurysms have formed at LCx #11 (**b**) and RCA #4PD (**c**).

BMS was implanted in LAD #7, and restudy performed half a year later found no evidence of restenosis. Thus, administration of ticlopidine was discontinued, and only aspirin was continued to be administered, while observing the course. However, restenosis of the stent was detected at 4 months after the restudy. Redilation was achieved by plain old balloon angioplasty (POBA), and the patient was put on oral aspirin, ticlopidine, diltiazem and nicorandil, but after about half a year the stent once again became occluded. A DES (Cypher stent) was implanted proximal to, and overlapping the BMS. However, stent thrombosis developed 3 days after implantation of the DES, and recanalization was achieved by aspirating the thrombus. The patient was asymptomatic for 7 months thereafter, but then chest pain occurred and required readmission to the hospital. Reocclusion of the stent at LAD #7 and new occlusion at RCA #4AV were found. The thrombus at LAD #7 was aspirated, and a second DES (Cypher stent) was implanted in the proximal portion of the existing stents. For the occlusion at RCA #4AV, thrombus aspiration and POBA were performed, but adequate dilation was unable to be achieved. There were initially no symptoms thereafter, but at 5 months after the implantation of the second DES (Cypher stent) the patient suddenly experienced chest pain and lost consciousness. The patient was in a state of ventricular fibrillation when the emergency medical assistance team arrived, did not respond to cardiopulmonary rescue and died.

During observation, the patient had shown no evidence of a condition that could serve as the cause of thrombosis, such as collagen disease, anti-phospholipid antibody syndrome or coagulation disorder. However, possible anamnesis of Kawasaki disease was suspected from the time of the first episode of acute myocardial infarction since lesions accompanied by aneurysms were observed in the coronary arteries. However, such a history was unable to be firmly established. The possibility of metal allergies was also considered, and for that reason a patch test was performed; the results showed allergic reactions to iron, nickel and chrome. A blood workup did not reveal hypereosinophilia, and the patient had no history of asthma.

Pathological findings

The weight of the heart was 330 g. Gross observation showed the LAD to be whitish in color and rigid, while RCA #4 was dilated to a diameter of approximately 7 mm and included a saccular aneurysm. At the distal portion of aneurysm at RCA #4, the blood vessel was whitish in color like the LAD and serpentine in its course (Fig. 2). In cross-section, extensive fibrosis was seen in the anterior wall septum and the posterior wall, in addition to scattered granulation tissue in the posterior wall and fresh infarction in the anterior and posterior walls.

In the left coronary artery, aneurysms, each having a diameter of approximately 7 mm, had formed at LCx #11 and LAD #6 (Figs. 3,4). These were true saccular aneurysms, and rupture of the internal elastic lamina was observed almost completely around the wall of the aneurysm, while the tunica media had become indistinct. In addition, fibrin thrombi and organized thrombi accompanied by fibrosis and calcification were observed in the aneurysm walls. Hardly any inflammatory cell infiltration was seen in the aneurysm walls. Three stents, having a total length of about 3 cm, had been implanted in the distal portion of the aneurysm in LAD #6. A BMS that had been implanted first occupied #7–8, while one DES each had been implanted at #7 and #8 so as to overlap the BMS. When the coronary artery where the metal stents were implanted was cut with scissors and a surgical knife, several fragments of the metal stent were exposed on the cut surface. The exposed metal stents were pulled out with tweezers carefully so as not to damage the surrounding tissues of

Lee, D.W., Wu, X., Eisenberg, E. & Greene, L.E. (2006) Recruitment dynamics of GAK and auxilin to clathrin-coated pits during endocytosis. *J. Cell Sci.* **119**, 3502–3512.

Lee, D.W., Zhao, X., Yim, Y.I., Eisenberg, E. & Greene, L.E. (2008) Essential Role of GAK (auxilin-2) in Developing and Mature Mice. *Mol. Biol. Cell* **19**, 2766–2776.

Lee, D.W., Zhao, X., Zhang, F., Eisenberg, E. & Greene, L.E. (2005) Depletion of GAK/auxilin 2 inhibits receptor-mediated endocytosis and recruitment of both clathrin and clathrin adaptors. *J. Cell Sci.* **118**, 4311–4321.

Lilyestrom, W., Klein, M.G., Zhang, R., Joachimiak, A. & Chen, X.S. (2006) Crystal structure of SV40 large T-antigen bound to p53: interplay between a viral oncoprotein and a cellular tumor suppressor. *Genes Dev.* **20**, 2373–2382.

Ohmori, K., Endo, Y., Yoshida, Y., Ohata, H., Taya, Y. & Enari, M. (2008) Monomeric but not trimeric clathrin heavy chain regulates p53-mediated transcription. *Oncogene* **27**, 2215–2227.

Okamoto, K. & Beach, D. (1994) Cyclin G is a transcriptional target of the p53 tumor suppressor protein. *EMBO J.* **13**, 4816–4822.

Okamoto, K., Kamibayashi, C., Serrano, M., Prives, C., Mumby, M.C. & Beach, D. (1996) p53-dependent association between cyclin G and the B′ subunit of protein phosphatase 2A. *Mol. Cell. Biol.* **16**, 6593–6602.

Okamoto, K., Li, H., Jensen, M.R., Zhang, T., Taya, Y., Thorgeirsson, S.S. & Prives, C. (2002) Cyclin G recruits PP2A to dephosphorylate Mdm2. *Mol. Cell* **9**, 761–771.

Ray, M.R., Wafa, L.A., Cheng, H., Snoek, R., Fazli, L., Gleave, M. & Rennie, P.S. (2006) Cyclin G-associated kinase: A novel androgen receptor-interacting transcriptional coactivator that is overexpressed in hormone refractory prostate cancer. *Int. J. Cancer* **118**, 1108–1119.

Reimer, C.L., Borras, A.M., Kurdistani, S.K., Garreau, J.R., Chung, M., Aaronson, S.A. & Lee, S.W. (1999) Altered regulation of cyclin G in human breast cancer and its specific localization at replication foci in response to DNA damage in $p53^{+/+}$ cells. *J. Biol. Chem.* **274**, 11022–11029.

Stanek, D. & Neugebauer, K.M. (2006) The Cajal body: a meeting place for spliceosomal snRNPs in the nuclear maze. *Chromosoma* **115**, 343–354.

Tamura, K., Kanaoka, Y., Jinno, S., Nagata, A., Ogiso, Y., Shimizu, K., Hayakawa, T., Nojima, H. & Okayama, H. (1993) Cyclin G: a new mammalian cyclin with homology to fission yeast Cig1. *Oncogene* **8**, 2113–8.

Westermarck, J, & Hahn. W.C. (2008) Multiple pathways regulated by the tumor suppressor PP2A in transformation. *Trends Mol. Med.* **14**, 152–160.

Zhang, C.X., Engqvist-Goldstein, A.E., Carreno, S., Owen, D.J., Smythe, E. & Drubin, D.G. (2005) Multiple roles for cyclin G-associated kinase in clathrin-mediated sorting events. *Traffic* **6**, 1103–1113.

Zhang, L., Gjoerup, O. & Roberts, T.M. (2004) The serine/threonine kinase cyclin G-associated kinase regulates epidermal growth factor receptor signaling. *Proc. Natl. Acad. Sci. USA* **101**, 10296–10301.

Received: 11 October 2008
Accepted: 19 February 2009

Supporting Information/Supplementary material

The following Supporting Information can be found in the online version of the article:

Figure S1 Subcellular localization of GAK and nuclear proteins.

Table S1 List of oligonucleotide sequences used for PCR amplification

Additional Supporting Information may be found in the online version of this article.

Please note: Wiley-Blackwell are not responsible for the content or functionality of any supporting materials supplied by the authors. Any queries (other than missing material) should be directed to the corresponding author for the article.

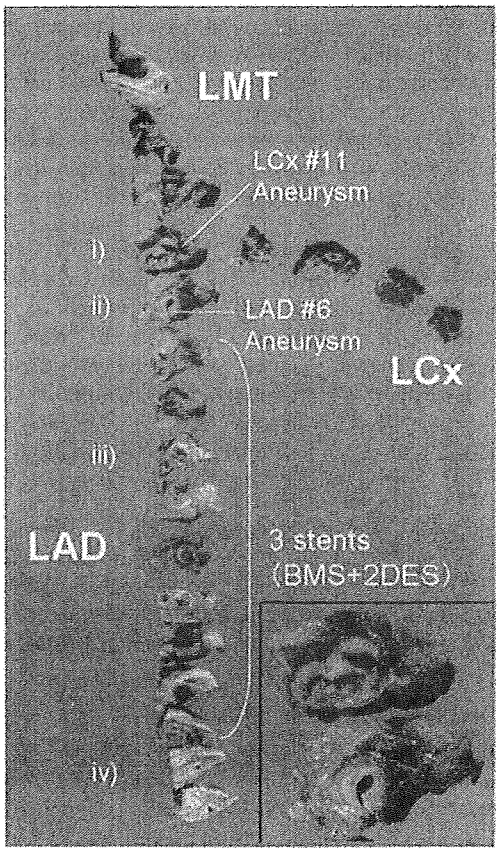

Figure 3 Cross-sections of the left coronary artery. Aneurysms had formed at LCx #11 and LAD #6 immediately posterior to the LMT-LCx bifurcation. Three stents, having a total length of 3 cm, had been implanted in the distal portion of the aneurysm at LAD #6. The first stent to be implanted, a BMS, had been placed at #7–8, and later one DES each was implanted at #7 and #8 so that they would overlap the BMS. (inset: Magnification of i and ii).

stents at several months after their implantation, whereas there are only very small numbers of eosinophils.[4,5] Our exhaustive search of the published literature revealed a total of only five reported cases of infiltration by numerous eosinophils, confined to the stent implantation site. Those cases were reported by Virmani *et al.*[6] Nebeker *et al.*[7] and Kawano *et al.*[8] Four of those patients died due to ST. Virmani *et al.* and Nebeker *et al.* autopsied two patients who died of LST that occurred after DES implantation and reported pathological findings at the stent implantation site that were very similar to those for our present patient. There is still little known regarding the mechanism by which eosinophils are involved in thrombus formation. However, there has been speculation regarding a possible mechanism in which major basic protein (MBP), which is included in acidophilic granules, binds to and inactivates thrombomodulin that is present on the vascular endothelium,[9] as well a possible mechanism in which hypothiocyanous acid (HOSCN) that is produced by eosinophil peroxidase causes a large increase in endothelial cell tissue factor activity.[10]

Metals, sirolimus and its coating polymers are considered to be substances with the potential to cause LST at sites of BMS or DES implantation.[6] Metal allergy has been looked upon as a potential problem since the time when BMS was first used. Koster *et al.*[11] reported that metal allergy develops in 10% of BMS implantation patients. In addition, they pointed out that the incidence of restenosis is higher in patients yielding positive patch test results for nickel and molybdenum, which are the stainless components of stents, compared with in patients showing negative patch test results. However, Virmani *et al.*[6] wrote that, although a hypersensitivity reaction in relation to BMS is involved in stent restenosis, there are no reports of associated formation of thrombi. They also reviewed more than 400 autopsy cases in which a BMS had been implanted, but they found no infiltration by eosinophils at the stent implantation site and thus surmised that those findings ruled out involvement of a hypersensitivity reaction due to stent metal components.[6] Moreover, the same group noted that sirolimus itself inhibits eosinophil infiltration while its incidence of hypersensitivity reactions is lower than the incidences seen with other drugs. They therefore surmised that the polymers have the strongest potential to be involved in the causation of LST after DES implantation.[6] It can be thought that in our present case, in which BMS and DES were implanted in an overlapping state, there was a real possibility of occurrence of a hypersensitivity reaction in relation to the polymers. However, the first episode of stent occlusion occurred at 10 months after implantation of the BMS, which did not contain any polymers, and the patch test at that time confirmed the patient to be allergic to nickel. This latter fact means that we cannot completely rule out the possibility that a metal allergy was involved in the LST seen in this patient.

When discussing the possible causes of the ST seen in our patient, it is necessary to consider not only a hypersensitivity reaction in relation to the stent but also the existence of post-inflammatory changes, especially the coronary aneurysms. In the LAD, the stent was implanted on the distal side of the coronary aneurysm. When an aneurysm is present, it is known that the patient is susceptible to falling into a state that is very conducive to thrombus formation due to stasis of the blood flow, activation of various coagulation factors such as the platelets, damage to the vascular intima, etc. Because of the added possibility of a hypersensitivity reaction in this patient, we surmised that the presence of the aneurysm might have induced the thrombus formation in the stent.

The coronary arteries in this patient showed destruction of the arterial architecture, including aneurysm formation, and it was surmised that vasculitis was involved in the causation of these changes. Vasculitis involving mainly the medium-size muscular arteries is seen in such diseases as Kawasaki

array analysis in cardiomyocytes also demonstrated that Lcn2/NGAL was a protein that was strongly induced in cardiomyocytes purified from rats with experimental autoimmune myocarditis (EAM).[15] It is known also that interleukin-1 (IL-1) plays an important role[16,17] and is highly expressed in hearts with myocarditis,[18,19] and because IL-1 induces Lcn2/NGAL expression,[6,14] we surmised that the Lcn2/NGAL mRNA level might also be increased in hearts with myocarditis. Accordingly, we investigated the expression of Lcn2/NGAL in rat EAM and in human myocarditis.

Methods

Animals

Male Lewis rats were obtained from Charles River, Japan (Atsugi, Kanagawa, Japan) and were maintained in our animal facilities until they reached 8 weeks of age in preparation for the EAM experiments. Throughout the studies, all animal experiments in our institute followed the guidelines for the care and use of laboratory animals published by the US National Institutes of Health.

Induction of EAM

Cardiac myosin was prepared from the ventricular muscle of porcine hearts as previously described.[20] To produce EAM each rat was immunized on day 0 with 0.2 ml of an emulsion containing porcine cardiac myosin, along with an equal volume of complete Freund's adjuvant supplemented with 10 mg/ml of Mycobacterium tuberculosis H37RA (Difco, Detroit, MI, USA).

Purification of Cells From EAM Hearts

EAM rats were killed on day 18. For analysis of Lcn2/NGAL and its specific receptor (24p3R) gene expressing cells, fractions of cardiomyocytes (n=5), $\alpha\beta$ T cells (n=5), CD11bc$^+$ cells (n=5) and non-cardiomyocytic non-inflammatory (NCNI) cells (mainly fibroblasts, smooth muscle cells, and endothelial cells) (n=6) were isolated and purified as previously described.[20] Cells from both ventricles were isolated by collagenase perfusion treatment for 20 min using a Langendorff apparatus. The isolated cells were serially separated through 38-μm stainless steel sieves to yield cardiomyocytes, and then through 20-μm sieves to yield non-cardiomyocytic (NC) cells. Because almost all inflammatory cells in EAM are $\alpha\beta$ T cells and CD11bc$^+$ cells, the NC cells were further separated into $\alpha\beta$ T cells, CD11bc$^+$ cells and NCNI cells, such as fibroblasts, smooth muscle cells or endothelial cells, with anti-PE micro beads (Miltenyi Biotec, Bergisch Gladbach, Germany) and a MACS magnetic cell sorting system (Miltenyi Biotec). For this process appropriate monoclonal antibodies, namely PE-conjugated TCR $\alpha\beta$ (R73) and CD11bc (OX-42) (Pharmingen, San Diego, CA, USA), were used.

RNA Extraction and Real-Time Reverse Transcriptase-Polymerase Chain Reaction (RT-PCR)

To examine the time course of Lcn2/NGAL and IL-1β expression in hearts, a group of 8-week old normal rats (n=3) was killed, and their results compared with EAM rats killed on days 9, 12, 15, 18, 30 (n=3 for each) and 60 (n=4). In each case a small part of the cardiac ventricle was extracted. A separate group of EAM rats was killed on day 13, and in each a small part of the cardiac ventricle, liver, spleen and kidney (n=4 in each group) was extracted to examine local Lcn2/NGAL expression in comparison with 8-week old normal rats and control rats injected with adjuvant alone. Total RNA was isolated from the materials described above using Trizol (Invitrogen, Tokyo, Japan). Synthesis of cDNA was carried out using 2–5 μg of total RNA with random primers and murine Moloney leukemia virus reverse transcriptase. To create the plasmids used for the standard, rat Lcn2/NGAL, rat 24p3R, rat IL-1β, and human Lcn2/NGAL mRNA were amplified from EAM heart or myocarditis autopsy specimen-derived cDNA using the primer pairs (rat-Lcn2/NGAL, sense primer 5'-gactcaactcagaacttgatccct-3' and antisense primer 5'-agctctgtatctgagggtagctgt-3'; rat-24p3R, sense primer 5'-ctaccgaaacatctggaaaaatct-3' and antisense primer s'-gtactgaggatagcagaagcttgg-3'; human-Lcn2/NGAL, sense primer 5'-tgagctgaaagaagacaagagcta-3' and antisense primer 5'-gatgaagttctcctttagttccga-3') and the primers as reported previously.[16] PCR-amplified cDNA inserts were directly inserted into the pGEM-T easy vector, and recombinant plasmids were isolated following transformation into *Escherichia coli* JM109-competent cells using a MagExtractor plasmid kit (Toyobo, Osaka, Japan). Absolute copy numbers of their mRNA were also measured by quantitative real-time RT-PCR using a LightCycler instrument (Roche Diagnostics, Tokyo, Japan) together with the same primers and SYBR Premix Ex Taq (Takara, Otsu, Japan). After an initial denaturation step of 10 min at 95°C, a 3-step cycling procedure (denaturation at 95°C for 10 s, annealing at 62°C for 10 s, and extension at 72°C for 13 s) was used for 45 cycles. The absolute copy numbers of particular transcripts were calculated by LightCycler software using a standard curve approach.

Method for ELISA

To examine the time course of plasma concentrations of Lcn2/NGAL, IL-1β, and B-type natriuretic peptide (BNP), blood samples were obtained from the tail vein of 8-week old normal rats, and from control rats injected with adjuvant alone and EAM rats on days 9, 13, 17, 21, 25, 29, 33, 45 and 60 (n=4 for each). For the rats, plasma Lcn2/NGAL concentrations were determined with a Rat NGAL ELISA kit according to the manufacturer's instructions (BioPorto Diagnostics, Gentofte, Denmark), BNP concentrations were determined with a BNP-32 EIA kit according to the manufacturer's instructions (Phoenix Pharmaceuticals Inc, Burlingame, CA, USA), and IL-1β concentrations were determined with a Rat IL-1β ELISA kit according to the manufacturer's instructions (Pierce Biotechnology Inc, Rockford, IL, USA). Absorbance at 450 nm was measured, and concentrations determined by interpolation from a standard calibration curve.

Immunohistochemistry

Tissue samples were fixed at room temperature in 10% formalin. Samples from human hearts and the hearts of normal rats and those with EAM on day 17 were sequentially dehydrated through an alcohol series and embedded in paraffin. Sections 4-μm thick were cut, deparaffinized in xylene, and dehydrated in descending dilutions of ethanol. Specimens were treated by incubating them in EDTA (pH 8.0) buffer at 121°C for 15 min in an autoclave. After washing in 0.01 mol/L phosphate-buffered saline (PBS), endogenous peroxidase activity was blocked by treatment for 20 min with 0.3% hydrogen peroxidase in absolute methanol. Specimens were incubated with 10% normal goat serum for 10 min at room temperature and for both rats and humans they were reacted with rabbit anti-Lcn2/NGAL antibody (abcam, Cambridge, UK) overnight at 4°C. The samples were then incubated for 2 h at room temperature with appropriate second-